Dual Tracer Autoradiographic Study with Thallium-201 and Radioiodinated Fatty Acid in Cardiomyopathic Hamsters

Chinori Kurata, Akira Kobayashi, and Noboru Yamazaki

The Third Department of Internal Medicine, Hamamatsu University School of Medicine, Hamamatsu, Japan.

To investigate the usefulness of myocardial scintigraphy with radioiodinated 15-(p-iodophenyl)-3-R,S-methylpentadecanoic acid (BMIPP) in cardiomyopathy, quantitative dual tracer autoradiographic study with ^{201}Tl and [^{125}I]BMIPP was performed in 27 cardiomyopathic Bio 14.6 Syrian hamsters and eight normal hamsters. Furthermore, 16 Bio 14.6 Syrian hamsters aged 21 days were divided into verapamil-treated (during 70 days) and control groups (respectively, n=8), and autoradiography with ^{201}Tl and [^{125}I]BMIPP was performed. Quantitative autoradiography demonstrated an uncoupling of ^{201}Tl and [^{125}I]BMIPP distributions and a regional heterogeneity of [^{125}I]BMIPP distribution in cardiomyopathic hamsters aged more than 2 mo, while normal hamsters showed only mild heterogeneity of [^{125}I]BMIPP distribution without an uncoupling of tracers. Age-matched comparison between normal and cardiomyopathic hamsters (5–8 mo old) demonstrated that a difference between their [^{125}I]BMIPP distributions are more marked than that between their ^{201}Tl distributions. Furthermore, [^{125}I]BMIPP visualized effects of verapamil on cardiomyopathy more distinctly than did ^{201}Tl. In conclusion, myocardial imaging with [^{123}I]BMIPP could be useful for investigating cardiomyopathy and evaluating the efficacy of therapeutic intervention in patients with cardiomyopathy.

J Nucl Med 30:80–87, 1989

Primary cardiomyopathies have been classified and recognized on the basis of anatomic and functional abnormalities regardless of the underlying metabolic processes. Biochemical studies by means of positron emission tomography have been expected not only to enhance our understanding of cardiomyopathies as well as their detection and characterization, but also to aid in the development of effective treatment (*1–3*). Various radiolabeled fatty acids have been proposed as means for detecting metabolic alterations of the myocardium in patients with cardiomyopathy as well as coronary artery disease (*4*). Among these fatty acids, the physiologic carbon-11 (^{11}C) palmitate with positron emission tomography has been considered an accurate agent for the quantitation of regional myocardial fatty acids utilization (*5*). However, the major limitation of positron imaging is the worldwide scarcity of the relatively expensive imaging devices and cyclotrons. Therefore, attention has been focused on gamma-emitting radionuclides labeled to fatty acids. For example, several radioiodinated fatty acids have been used for investigating accumulation and turnover of fatty acids in the myocardium of patients with cardiomyopathy (*6–8*).

Radioiodinated 15-(p-iodophenyl)-3-R,S-methylpentadecanoic acid (BMIPP) is a new myocardial imaging agent (*9*). BMIPP is obtained by attaching an iodide label to a benzene ring located at the omega-end of a pentadecanoic acid molecule, to avoid in vivo deiodination (*10*), and by inserting a methyl radical in the beta-position to inhibit beta-oxidation and prolong myocardial retention (*11*) (Fig. 1). BMIPP showed much longer myocardial retention than did the straight chain 15-(p-iodophenyl)-pentadecanoic acid in rats and human beings (*12,13*).

A recent quantitative dual tracer autoradiographic study performed in hypertensive rats revealed a dissociation between regional perfusion assessed by thallium-

Received Apr. 20, 1988; revision accepted Aug. 31, 1988.

For reprints contact: Chinori Kurata, MD, The Third Department of Internal Medicine, Hamamatsu University School of Medicine, 3600 Handa-cho, Hamamatsu, 431-31 Japan.

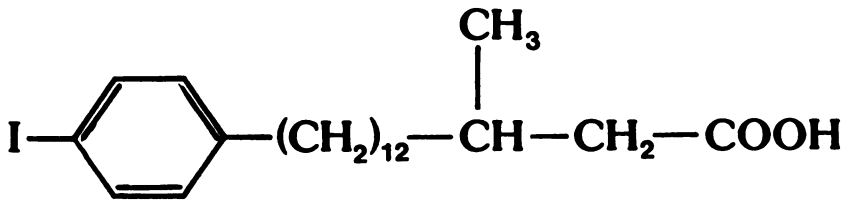

FIGURE 1
15-(p-iodophenyl)-3-R,S-methylpentadecanoic acid (BMIPP). An iodide label to a benzene ring located at the omega-end avoids in vivo deiodination, and a methyl radical in the beta-position inhibits beta-oxidation and prolong myocardial retention.

201 (^{201}Tl) and regional fatty acid utilization assessed by [1-^{14}C]-3-R,S-methylheptadecanoic acid in the myocardium (*14*). Such an uncoupling of regional perfusion and fatty acid utilization might exist in the myocardium of primary cardiomyopathy.

The Bio 14.6 Syrian hamster develops a hereditary cardiomyopathy terminating in congestive heart failure and provides a good model for the experimental study of cardiomyopathy (*15–17*). In this strain, myocardial oxidation of fatty acids has been reported to be substantially decreased (*18*). During ~1 mo of age, the animals appear well and there is no pathological evidence of disease. At ~1 mo, focal myocardial necrotic lesions appear. At about 3 to 4 mo of age, many of the necrotic lesions have healed, few new lesions appear, hypertrophy of the heart begins and calcification of the degenerating muscle appears. After about 6 mo of age, marked cardiac dilation appears and many animals die from congestive heart failure (*15–17,19*). In addition, verapamil, a calcium antagonist, has been reported to inhibit the progression of myocardial damages in the Bio 14.6 Syrian hamsters (*20–23*).

The present study was primarily concerned with the usefulness of BMIPP imaging in cardiomyopathy. For this purpose, we performed quantitative dual tracer autoradiographic study with ^{201}Tl and [^{125}I]BMIPP in the Bio 14.6 Syrian hamsters and, also, investigated the question of whether BMIPP imaging can detect the therapeutic effect of verapamil on cardiomyopathy.

METHODS

Radiopharmaceutical

Injectable solution of [^{125}I]BMIPP was obtained from Nihon Medi-Physics Co., Ltd., Chiba, Japan. The method of the preparation of [^{125}I]BMIPP was as follows. Commercially obtained BMIPP (EMKA Chemie GmbH, Markgroenigen-Talhausen, West Germany), was labeled with iodine-125 (^{125}I) by isotope exchange reaction using acetic acid as a solvent and $CuSO_4$ as a catalyst. The radiochemical yield was over 95% which determined by thin layer chromatography, and the specific activity ranged between 0.50 and 2.16 Ci/mmol. The crude product was purified by solvent extraction, and identified by the thin layer chromatography. The radiochemical purity of this purified product was nearly 100%. The labeled product was evaporated to dryness and dissolved into 6% HSA saline solution (ethanol free preparation). The solution was finally sterilized by Millipore (0.22 μm) filtration.

Dual Tracer Autoradiography in Cardiomyopathic and Normal Hamsters

Twenty-seven Bio 14.6 Syrian hamsters were divided into four age groups, namely, five animals aged 1 mo, six animals aged 2 to 2.5 mo, seven animals aged 3 to 5 mo and nine animals aged 6 to 12 mo. Eight normal golden hamsters, aged 5 to 8 mo, were used as controls.

All animals were first injected intravenously with 16 μCi to 64 μCi of [^{125}I]BMIPP, then 20 min later with 160 to 640 μCi of ^{201}Tl. The dose ratio of [^{125}I]BMIPP and ^{201}Tl (μCi) was 1/10 in all animals. The hearts were removed 10 min after the second injection, frozen in liquid nitrogen, embedded in carboxy-methyl-cellulose, and sectioned in the direction perpendicular to the longitudinal axis of the left ventricle with a cryomicrotome. The myocardial sections of 20-μm thickness and graded standards were placed on x-ray films for exposure. The first autoradiographic exposure was carried out for 11 hr to reveal the thallium distribution. The second exposure was initiated 30 days later following the decay of ^{201}Tl activity and the imaging of [^{125}I]BMIPP required 30 days for adequate image quality. In the single tracer autoradiography of each tracer under the same condition as that of the dual tracer autoradiography, it was confirmed that ^{201}Tl images were not visualized under the condition of exposure for imaging [^{125}I] BMIPP uptake and that [^{125}I]BMIPP images were not visualized under the condition of exposure for imaging ^{201}Tl uptake.

To quantitate myocardial distributions of ^{201}Tl and [^{125}I] BMIPP, a myocardial section was divided into five regions, that is, the right ventricular wall, the right ventricular side of the interventricular septum, the left ventricular side of the interventricular septum, the endocardial region of the left ventricular free wall, and the epicardial region of the left ventricular free wall. These selected regions of ^{201}Tl and ^{125}I autoradiograms were digitized and quantitated using a videodensitometric system, a CCD camera (Sony, Japan) with an image processor (TOSPIX, Toshiba, Japan) (*24*). For each region, the relative uptake of the tracer was defined as the ratio of the regional optical density to the maximum optical density in the five regions. It was confirmed, using graded standards exposed and digitized under the same condition as heart images, that regional optical densities measured by a videodensitometric system in this study were within the range of linear relation to tissue tracer concentrations. Therefore, the relative uptake defined above reflects the relative distribution of the tracer in the myocardium and affords the information on the clinical availability of [^{123}I]BMIPP imaging using conventional gamma camera system because of the relatively large size of selected regions.

Detection of Effects of Verapamil by Autoradiography

Sixteen Bio 14.6 Syrian hamsters aged 21 days were divided into two groups and treated as follows. Eight verapamil-treated

animals were injected intraperitoneally with 5 mg/kg of verapamil twice daily during the 21th to 90th day of life. Eight saline-treated animals were injected with the same volumes of physiological saline solution during the same period as verapamil-treated group. All animals were killed at age 90 days and quantitative dual tracer autoradiography was carried out using ^{201}Tl and [^{125}I]BMIPP as described above. It has been already reported by our group that such early treatment with verapamil protects against histopathological damages in the myocardium of the Bio 14.6 Syrian hamsters (*25*).

Statistical Analysis

All values of relative uptakes were expressed as mean ± standard deviation. Comparisons of ^{201}Tl and [^{125}I]BMIPP were performed by the paired, two-tailed Student's t-test. Intergroup comparisons were performed by the unpaired, two-tailed Student's t-test. One-way analysis of variance was used to compare relative uptakes among the five regions for each tracer and each group. A p value greater than or equal to 0.05 was considered to indicate the lack of a significant difference.

RESULTS

Dual Tracer Autoradiography in Cardiomyopathic and Normal Hamsters (Fig. 2, Table 1 and 2)

As examples shown in Figure 2, in the control hamster, the ^{201}Tl distribution was uniform and the [^{125}I] BMIPP distribution was also uniform except for a slightly low uptake in the endocardial region of the left ventricle. By contrast, in the Bio 14.6 Syrian hamster aged 11 mo, the ^{201}Tl distribution showed diffusely scattered small defects, and the BMIPP distribution was decreased in the right ventricular wall, interventricular septum and endocardial region of the left ventricular free wall. As shown in Table 1, in the control group and Bio 14.6 Syrian hamsters aged 1 mo, the relative uptakes of ^{201}Tl and [^{125}I]BMIPP did not significantly differ in any of the regions. In the Bio 14.6 Syrian hamsters aged 2 to 2.5 mo, however, [^{125}I]BMIPP uptake was significantly lower than that of ^{201}Tl in the left ventricular side of the interventricular septum ($p < 0.01$) and right ventricular wall ($p < 0.05$). Furthermore, in the Bio 14.6 Syrian hamsters aged 3 to 5 and 6 to 12 mo, [^{125}I]BMIPP uptake was significantly lower than that of ^{201}Tl in the right ventricular wall ($p < 0.01$) and endocardial region of the left ventricular free wall ($p < 0.01$) as well as the left ventricular side of the interventricular septum ($p < 0.01$). Relative uptakes of ^{201}Tl were not significantly different among five regions in any groups of cardiomyopathic hamsters ($p > 0.05$) as well as the control group ($p > 0.05$). By contrast, relative uptakes of [^{125}I]BMIPP among five regions were slightly but significantly different in the control group ($p < 0.05$) and markedly different in the cardiomyopathic hamsters aged more than 2 mo ($p < 0.01$).

Eight animals of the same age as the control group, that is, 5 to 8 mo old were selected from 27 Bio 14.6 Syrian hamsters and the age-matched comparison between control and Bio 14.6 Syrian hamsters was performed. As shown in Table 2, ^{201}Tl uptake in the left ventricular side of the interventricular septum of the

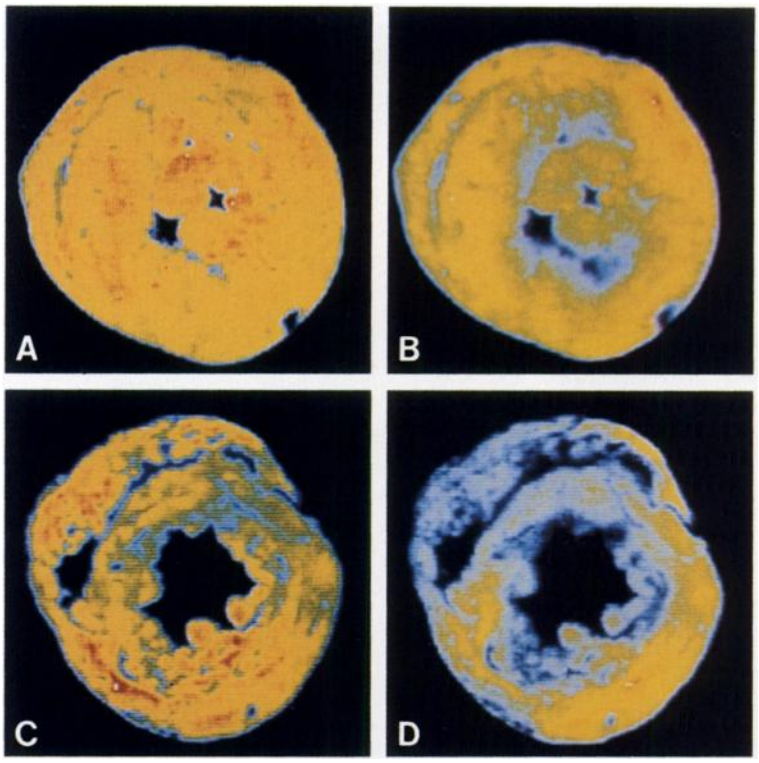

FIGURE 2
Illustrative digitized dual tracer autoradiograms with ^{201}Tl and [^{125}I] BMIPP in the control and cardiomyopathic hamsters. A ^{201}Tl autoradiogram of a 8-mo-old normal hamster shows uniform distribution (A). A [^{125}I]BMIPP autoradiogram of the same section as A shows uniform distribution except for a slightly low uptake in the endocardial region of the left ventricle (B). A ^{201}Tl autoradiogram of a 11-mo-old Bio 14.6 Syrian hamster shows diffusely scattered small defects (C). A [^{125}I]BMIPP autoradiogram of the same section as C shows decreased uptakes in the right ventricular wall, interventricular septum and endocardial region of the left ventricular free wall (D).

TABLE 1
Relative Uptakes in Control and Cardiomyopathic Hamsters

Groups	Tracers	Regions					p Values†
		RV	SepR	SepL	LVendo	LVepi	
Control	^{201}Tl	0.93 ± 0.07	0.96 ± 0.03	0.97 ± 0.04	0.93 ± 0.03	0.95 ± 0.04	N.S.
	[^{125}I]BMIPP	0.91 ± 0.05	0.95 ± 0.05	0.90 ± 0.06	0.87 ± 0.07	0.97 ± 0.05	<0.05
Bio (1 mo)	^{201}Tl	0.85 ± 0.14	0.93 ± 0.05	0.92 ± 0.09	0.94 ± 0.08	0.95 ± 0.06	N.S.
	[^{125}I]BMIPP	0.88 ± 0.09	0.93 ± 0.07	0.98 ± 0.03	0.95 ± 0.04	0.95 ± 0.04	N.S.
Bio (2-2.5 mo)	^{201}Tl	0.93 ± 0.06	0.96 ± 0.04	0.92 ± 0.05	0.95 ± 0.08	0.91 ± 0.07	N.S.
	[^{125}I]BMIPP	0.86 ± 0.09*	0.94 ± 0.03	0.78 ± 0.08‡	0.82 ± 0.13	0.99 ± 0.02*	<0.01
Bio (3–5 mo)	^{201}Tl	0.88 ± 0.08	0.94 ± 0.08	0.91 ± 0.10	0.94 ± 0.07	0.95 ± 0.09	N.S.
	[^{125}I]BMIPP	0.67 ± 0.10‡	0.85 ± 0.09	0.69 ± 0.05‡	0.70 ± 0.13‡	0.99 ± 0.02	<0.01
Bio (6–12 mo)	^{201}Tl	0.93 ± 0.12	0.89 ± 0.07	0.87 ± 0.05	0.95 ± 0.05	0.94 ± 0.06	N.S.
	[^{125}I]BMIPP	0.67 ± 0.11‡	0.82 ± 0.13*	0.68 ± 0.09‡	0.73 ± 0.13‡	1.00 ± 0.01*	<0.01

Values are means ± standard deviation. The significance of the differences is as follows: ^{201}Tl versus [^{125}I]BMIPP, * $p < 0.05$, ‡ $p < 0.01$; † refers to comparisons among relative uptakes in five regions (one-way analysis of variance). Bio (x mo) = Bio 14.6 Syrian hamsters (x months old); BMIPP = 15-(p-iodophenyl)-3-R,S-pentadecanoic acid; Control = control hamsters; LVendo = endocardial region of the left ventricular free wall; LVepi = epicardial region of the left ventricular free wall; N.S. = not significant ($p > 0.05$); RV = right ventricular wall; SepL = left ventricular side of the septum; SepR = right ventricular side of the septum.

Bio 14.6 Syrian hamsters was slightly but significantly lower than that in the same region of the control group ($p < 0.05$). By contrast, the Bio 14.6 Syrian hamsters displayed a significantly low uptake of [^{125}I]BMIPP in the right ventricular wall ($p < 0.01$), endocardial region of the left ventricular free wall ($p < 0.01$), left ventricular side of the septum ($p < 0.01$) and right ventricular side of the septum ($p < 0.05$), as compared with the control group.

Detection of Effects of Verapamil by Dual Tracer Autoradiography (Fig. 3 and Table 3)

As examples shown in Figure 3, in the saline group, both ^{201}Tl and [^{125}I]BMIPP demonstrated diffusely scattered small defects as well as decreased [^{125}I]BMIPP uptake in the right ventricular wall, septum, and endocardial region of the left ventricular free wall. By contrast, neither defects nor reduced regional uptakes of either tracer were detectable in the verapamil group. Table 3 shows the comparison between the saline and verapamil groups with respect to the relative uptakes of each tracer. The ^{201}Tl distribution of the saline and verapamil groups did not differ in any of the regions ($p > 0.05$). By contrast, the relative uptake of [^{125}I]BMIPP in the left ventricular side of the interventricular septum was significantly greater in the verapamil group than in the saline group ($p < 0.05$). In the saline group, relative uptakes of ^{201}Tl were slightly but significantly different

TABLE 2
Age-Matched Comparison of Relative Uptakes in Control and Cardiomyopathic Hamsters

Tracers	Groups	Regions				
		RV	SepR	SepL	LVendo	LVepi
^{201}Tl	Control	0.93 ± 0.07	0.96 ± 0.03	0.97 ± 0.04	0.93 ± 0.03	0.95 ± 0.04
	Bio	0.93 ± 0.09	0.93 ± 0.04	0.89 ± 0.06*	0.95 ± 0.06	0.96 ± 0.06
[^{125}I]BMIPP	Control	0.91 ± 0.05	0.95 ± 0.05	0.90 ± 0.06	0.87 ± 0.07	0.97 ± 0.05
	Bio	0.67 ± 0.05†	0.83 ± 0.13*	0.69 ± 0.09†	0.71 ± 0.14†	1.00 ± 0.01

Values are means ± standard deviation. The significance of the difference is as follows: control versus Bio, * $p < 0.05$, † $p < 0.01$. Bio = Bio 14.6 Syrian hamsters aged 5–8 mo; Control = control hamsters aged 5–8 mo; other abbreviations are as in Table 1.

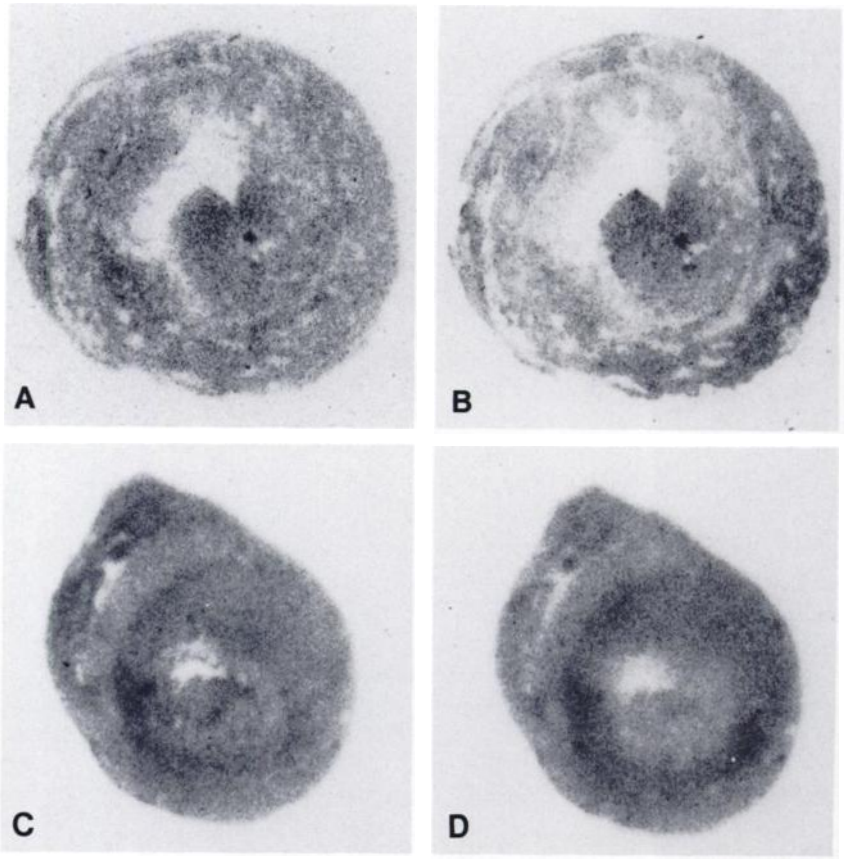

FIGURE 3
Illustrative dual tracer autoradiograms with ^{201}Tl and [^{125}I]BMIPP in the saline and verapamil groups. A ^{201}Tl autoradiogram of a saline-treated hamster shows diffusely scattered small defects (A). A [^{125}I] BMIPP autoradiogram of the same section as A shows decreased uptakes in the right ventricular wall, interventricular septum and endocardial region of the left ventricular free wall (B). Both a ^{201}Tl and [^{125}I] BMIPP autoradiograms (respectively, C and D) of a verapamil-treated hamster show neither defects nor reduced regional uptakes.

among five regions ($p < 0.05$) and relative uptakes of [^{125}I]BMIPP were markedly different among five regions ($p < 0.01$). By contrast, in the verapamil group, relative uptakes of either ^{201}Tl or [^{125}I]BMIPP showed no significant differences among five regions ($p > 0.05$).

DISCUSSION

Heterogeneity of [^{125}I]BMIPP Distribution

The myocardial distribution of [^{125}I]BMIPP in cardiomyopathic hamsters aged more than 2 mo was different from that of ^{201}Tl and also different from that of [^{125}I]BMIPP in normal hamsters. In normal hamsters, ^{201}Tl accumulation was homogeneous and [^{125}I]BMIPP accumulation was almost homogeneous other than slightly decreased uptake in the left ventricular side of the interventricular septum. In cardiomyopathic hamsters aged 1 mo, both ^{201}Tl and [^{125}I]BMIPP accumulations were homogeneous. In cardiomyopathic hamsters aged more than 2 mo, however, [^{125}I]BMIPP accumulation was highly heterogeneous with significantly decreased uptake in the endocardial region of the left ventricular free wall, left ventricular side of the interventricular septum and right ventricular wall. The older

TABLE 3
Comparison of Relative Uptakes in Saline and Verapamil Groups

Tracers	Groups	Regions					p Values†
		RV	SepR	SepL	LVendo	LVepi	
^{201}Tl	Saline	0.85 ± 0.12	0.88 ± 0.08	0.85 ± 0.08	0.91 ± 0.08	0.98 ± 0.03	<0.05
	Verapamil	0.89 ± 0.12	0.91 ± 0.06	0.85 ± 0.07	0.89 ± 0.06	0.93 ± 0.07	NS
[^{125}I]BMIPP	Saline	0.77 ± 0.11	0.87 ± 0.09	0.72 ± 0.09	0.87 ± 0.10	0.98 ± 0.03	<0.01
	Verapamil	0.84 ± 0.09	0.93 ± 0.13	0.84 ± 0.10*	0.86 ± 0.05	0.94 ± 0.06	NS

Values are means ± standard deviation. The significance of differences is as follows: saline versus verapamil, * $p < 0.05$; † refers to comparisons among relative uptakes in five regions (one-way analysis of variance). Saline = saline-treated hamsters; Verapamil = verapamil-treated hamsters; other abbreviations are as in Table 1.

the Bio 14.6 Syrian hamsters, the more distinctly the regional heterogeneity of myocardial distribution of [^{125}I]BMIPP.

^{201}Tl Autoradiograms

Numerous, small defects in ^{201}Tl autoradiograms, which were thought to reflect histologic changes of cardiomyopathy such as necrosis, fibrosis, and calcification, were observed in the Bio 14.6 Syrian hamsters of the late phase. These defects, however, were too small and too diffusely scattered to be detectable by the analysis of the regional relative uptake defined in this study. Therefore, if such alterations of ^{201}Tl and [^{125}I] BMIPP distributions as observed in the Bio 14.6 Syrian hamsters exist in patients with cardiomyopathy, abnormalities of [^{123}I]BMIPP distribution will be more feasible for visualization by single photon emission computed tomography (SPECT) than those of ^{201}Tl distribution. Namely, [^{123}I]BMIPP imagings with SPECT could be applied in human subjects to detect possible alterations in myocardial fatty acid metabolism in patients with cardiomyopathy of the early stage when no perfusion defects are detectable by ^{201}Tl imagings with SPECT.

Uncoupling of ^{201}Tl and [^{125}I]BMIPP Distributions

It has been reported that an uncoupling of myocardial distributions of ^{201}Tl and [1-^{14}C]-3-R,S-methylheptadecanoic acid occurs in hypertensive rats of the Dahl strain (*14*). Clinical study with positron emission tomography showed that [^{11}C]palmitate accumulation in the myocardium of patients with cardiomyopathy was highly heterogeneous and that such heterogeneity could not be explained by regional differences in myocardial perfusion assessed by ^{201}Tl scintigraphy (*2*). Subsequent study demonstrated that myocardial distribution of [^{131}I]BMIPP was essentially the same as that of 1[^{14}C]-3-R,S-methylheptadecanoic acid in normotensive and hypertensive rats (*26*). In our study, also, an uncoupling of ^{201}Tl and [^{125}I]BMIPP distributions was observed in the myocardium of the Bio 14.6 Syrian hamsters aged more than 2 mo. What does such an uncoupling of ^{201}Tl and radiolabeled fatty acid mean? Yonekura et al. (*14*) suggested that substrate utilization is altered in prolonged severe hypertension before ischemia occurs in hypertensive rats. In the Bio 14.6 Syrian hamsters, an uncoupling of myocardial distributions of ^{201}Tl and [^{125}I]BMIPP became more significant according to aging. A regional change in ^{201}Tl uptake was seen in a later phase and with a lower intensity than that in [^{125}I] BMIPP uptake. It is, therefore, suggested that regional fatty acid utilization could alter either independent of regional perfusion or before alterations of regional perfusion in the Bio 14.6 Syrian hamsters. If cardiomyopathy begins at the biochemical level and subsequently shows structural and anatomical impairments, myocardial imaging with radiolabeled fatty acids such as [^{123}I] BMIPP could play an important role in the diagnosis of cardiomyopathy of the early stage when myocardial perfusion or function is still normal.

Influence of Congestive Heart Failure

There is a possibility that the abnormality of myocardial distribution of [^{125}I]BMIPP in the Bio 14.6 Syrian hamsters may not be due to cardiomyopathy itself but due to congestive heart failure secondary to cardiomyopathy (*27,28*). The abnormality of [^{125}I] BMIPP distribution, however, was observed in the hamsters of the early phase, in which an overt heart failure is seldom observed (*16,17,19*). It is, therefore, unlikely that congestive heart failure alone could account for the abnormality observed in [^{125}I]BMIPP autoradiogram of the Bio 14.6 Syrian hamsters of the early phase. The abnormality of [^{125}I]BMIPP distribution in the late phase might be accelerated by congestive heart failure.

Evaluation of Effect of Verapamil

[^{125}I]BMIPP visualized the effects of verapamil on cardiomyopathy more distinctly than did ^{201}Tl. The uncoupling of ^{201}Tl and [^{125}I]BMIPP distributions observed in the saline group disappeared in the verapamil group. Verapamil may improve cardiomyopathy by preventing the toxic effects of calcium overload, and may also prevent focal damages by preventing microvascular spasm (*20,22,29*). The verapamil-induced homogeneity of [^{125}I]BMIPP distribution might be due to restoration of fatty acid metabolism secondary to inhibition of voltage-dependent calcium uptake (*30*). Numerous, small defects in ^{201}Tl autoradiograms also disappeared by treatment with verapamil. But, as mentioned above, these changes in ^{201}Tl autoradiograms which may reflect histopathological improvements could not be easily visualized by SPECT with ^{201}Tl. Therefore, SPECT study with [^{123}I]BMIPP may provide an efficient means of designing therapies to reserve or halt abnormal metabolic processes and evaluating the efficacy of therapeutic interventions in patients with cardiomyopathy.

Other Radioiodinated Phenyl Fatty Acids

Several radioiodinated phenyl fatty acids have been used in experimental and clinical studies (*8,13,31,32*). Especially, the straight chain 15-(p-iodophenyl)-pentadecanoic acid (IPPA) has been widely used in the evaluation of coronary artery disease (*31,32*). However, the myocardial distribution of [^{123}I]IPPA may change significantly during acquisition of SPECT because of the rapid oxidation and subsequent clearance from the myocardium (*13*). With respect to myocardial retention, 15-(p-iodophenyl)-3,3-dimethylpentadecanoic acid (DMIPP) has been reported to show longer retention than BMIPP as well as IPPA, because DMIPP is apparently not catabolized by the myocardium (*13,33*).

Recently, Kubota et al. (*34*) reported quantitative autoradiographic study with [^{131}I]DMIPP in the cardiomyopathic hamsters. Their result was almost similar to ours. However, the investigation of "regional relative uptakes" as performed in our study, which examined the clinical availability with SPECT, were not indicated in their study with [^{131}I]DMIPP. Furthermore, in the tissue distribution studies of [^{125}I]DMIPP in rats, Knapp et al. (*33*) have shown that the mean heart-to-liver ratios (% injected dose/g of tissue) are much less than 1 during 2 hr after injection. On the other hand, it has been reported that the heart level of [^{125}I]BMIPP (% injected dose/g of tissue) in rats is almost equal to the liver level at 30 min after injection and significantly higher than the liver level at 60 min after injection (*9*). Therefore, the liver level of DMIPP may be too high for clinical application of DMIPP to myocardial imaging.

Mechanisms of Myocardial Accumulation of BMIPP

It is still unclear whether regional alterations in the myocardial accumulation of [^{125}I]BMIPP is due to a defect in membrane transport, an impairment in energy production or utilization, or a reduction in the ratio of capillaries to sarcomeres. Ambrose et al. (*13*) have demonstrated that BMIPP shows primarily equal distribution in the mitochondrial, microsomal and cytoplasmic fractions and rapid incorporation into triglycerides. It is possible that myocardial retention of BMIPP represents not only beta-oxidation of fatty acids but also activity of myocardial uptake of fatty acids or esterification of fatty acids into neutral lipids. Nonetheless, since myocardial oxidation of [^{14}C]palmitate has been reported to be significantly depressed in the Bio 14.6 Syrian hamster (*18*), regional heterogeneity of myocardial distribution of BMIPP is likely to reflect regional impairments in fatty acid metabolism. Furthermore, since marked heterogeneity of myocardial distribution of [^{11}C]palmitate has been reported in patients with cardiomyopathy (*2*), myocardial imagings with BMIPP could be applied in patients with cardiomyopathy to detect possible alterations in fatty acid metabolism. While applying BMIPP to clinical studies, further experimental studies are needed to clarify the relationship between myocardial uptake of BMIPP and activity of beta-oxidation of fatty acids.

CONCLUSION

Our dual autoradiographic study demonstrated an uncoupling of ^{201}Tl and [^{125}I]BMIPP distributions in the myocardium of the Bio 14.6 Syrian hamsters aged more than 2 mo. Myocardial distribution of [^{125}I]BMIPP in the Bio 14.6 Syrian hamsters was significantly different from that in normal hamsters. The early treatment with verapamil restored the uncoupling of ^{201}Tl and [^{125}I]BMIPP distributions in the myocardium of the Bio 14.6 Syrian hamsters, and [^{125}I]BMIPP visualized the effects of verapamil on cardiomyopathy more distinctly than did ^{201}Tl. It is therefore suggested that myocardial imaging with [^{123}I]BMIPP could be useful for investigating cardiomyopathy and evaluating the efficacy of therapeutic intervention in patients with cardiomyopathy.

ACKNOWLEDGMENTS

The authors thank Yo Sakuma, PhD and Nihon Medi-Physics Co., Ltd. for the production of the isotopes, Ms. Shiomi Suzuki and Ms. Michiyo Sagisaka for assistance with daily injections with verapamil and saline solutions, and Hideshi Fujiwake, PhD and Mr. Yutaka Tsuchiya (Hamamatsu Photonics K.K., Japan) for assistance with the analysis with a videodensitometric system. This study was supported in part by grants-in-aid for encouragement of young scientists (62770584) from the Ministry of Education, Science and Culture, Japan.

REFERENCES

1. Schelbert HR, Phelps ME, Shine KJ. Imaging metabolism and biochemistry. *Am Heart J* 1984; 105:522–526.
2. Geltman EM, Smith JL, Beecher D, Ludbrook PA, Ter-Pogossian MM, Sobel BE. Altered regional myocardial metabolism in congestive cardiomyopathy detected by positron tomography. *Am J Med* 1983; 74:773–785.
3. Sochor H, Schelbert HR, Schwaiger M, Henze E, Phelps ME. Studies of fatty acid metabolism with positron emission tomography in patients with cardiomyopathy. *Eur J Nucl Med* 1986; 12:S66–S69.
4. van der Wall EE. Myocardial imaging with radiolabeled free fatty acids. In: Simoons ML, Reiber JHC, eds. Nuclear imaging in clinical cardiology. Boston: Martinus Nijhoff; 1984:83–102.
5. Weiss ES, Hoffman EJ, Phelps ME, et al. External detection and visualization of myocardial ischemia with ^{11}C-substrates in vitro and in vivo. *Circ Res* 1976; 39:24–32.
6. Hoeck A, Freundlieb C, Vyska K, Loesse B, Erbel R, Feinendegen LE. Myocardial imaging and metabolic studies with [17-^{123}I]iodoheptadecanoic acid in patients with idiopathic congestive cardiomyopathy. *J Nucl Med* 1983; 24:22–28.
7. Rabinovitch MA, Kalff V, Allen R, et al. ω-^{123}I-hexadecanoic acid metabolic probe of cardiomyopathy. *Eur J Nucl Med* 1985; 10:222–227.
8. Livni E, Elmaleh DR, Barlai-Kovach MM, Goodman MM, Knapp FF Jr, Strauss HW. Radioiodinated beta-methyl phenyl fatty acids as potential tracers for myocardial imaging and metabolism. *Eur Heart J* 1985; 6(Suppl B):85–89.
9. Goodman MM, Kirsch G, Knapp FF Jr. Synthesis and evaluation of radioiodinated terminal p-iodophenyl-substituted α- and β-methyl-branched fatty acids. *J Med Chem* 1984; 27:390–397.
10. Machulla HJ, Marsmann M, Dutschka K. Biochemical concept and synthesis of a radioiodinated phenyl-

fatty acid for in vivo metabolic studies of the myocardium. *Eur J Nucl Med* 1980; 5:171–173.
11. Livni E, Elmaleh DR, Levy S, Brownell GL, Strauss WH. Beta-methyl[1-^{11}C]heptadecanoic acid: a new myocardial metabolic tracer for positron emission tomography. *J Nucl Med* 1982; 23:169–175.
12. Dudczak R, Schmoliner R, Angelberger P, Knapp FF, Goodman MM. Structurally modified fatty acids: clinical potential as tracers of metabolism. *Eur J Nucl Med* 1986; 12:S45–S48.
13. Ambrose KR, Owen BA, Goodman MM, Knapp FF Jr. Evaluation of the metabolism in rat hearts of two new radioiodinated 3-methyl-branched fatty acid myocardial imaging agents. *Eur J Nucl Med* 1987; 12:486–491.
14. Yonekura Y, Brill AB, Som P, et al. Regional myocardial substrate uptake in hypertensive rats: a quantitative autoradiographic measurement. *Science* 1985; 227:1494–1496.
15. Homburger F, Baker JR, Nixon CW, Whitney R. Primary generalized polymyopathy and cardiac necrosis in an inbred line of Syrian hamsters. *Med Exp* 1962; 6:339–345.
16. Bajusz E, Baker JR, Nixon CW, Homburger F. Spontaneous hereditary myocardial degeneration and congestive heart failure in a strain of Syrian hamsters. *Ann NY Acad Sci* 1969; 156:105–129.
17. Bishop SP, Sole MJ, Tilley LP. Cardiomyopathies. In: Andrews EJ, Ward BC, Altman NH, eds. *Spontaneous models of human disease.* New York: Academic Press; 1979:59–64.
18. Kako KJ, Thornton MJ, Heggtveit HA. Depressed fatty acid and acetate oxidation and other metabolic defects in homogenates from hearts of hamsters with hereditary cardiomyopathy. *Circ Res* 1974; 34:570–580.
19. Gertz EW. Cardiomyopathic Syrian hamster: a possible model of human disease. *Prog Exp Tumor Res* 1972; 16:242–260.
20. Lossnitzer K, Janke J, Hein B, Stauch M, Fleckenstein A. Disturbed myocardial calcium metabolism: a possible pathogenetic factor in the hereditary cardiomyopathy of the Syrian hamster. *Recent Adv Stud Card Struct Metab* 1975; 6:207–217.
21. Jasmin G, Solymoss B. Prevention of hereditary cardiomyopathy in the hamster by verapamil and other agents. *Proc Soc Exp Bio Med* 1975; 149:193–198.
22. Factor SM, Minase T, Cho S, Dominitz R, Sonnenblick EH. Microvascular spasm in the cardiomyopathic Syrian hamster: a preventable cause of focal myocardial necrosis. *Circulation* 1982; 2:342–354.
23. Wikman-Coffelt J, Sievers R, Parmley WW, Jasmin G. Verapamil preserves adenine nucleotide pool in cardiomyopathic Syrian hamster. *Am J Physiol* 1986; 250:H22–H28.
24. Yonekura Y, Brill AB, Som P, Bennett GW, Fand I. Quantitative autoradiography with radiopharmaceuticals, part 1: digital film-analysis system by videodensitometry: concise communication. *J Nucl Med* 1983; 24:231–237.
25. Yamashita T, Kobayashi A, Yamazaki N, Miura K, Shirasawa H. Effects of L-carnitine and verapamil on myocardial carnitine concentration and histopathology of Syrian hamster Bio 14.6. *Cardiovasc Res* 1986; 20:614–620.
26. Yamamoto K, Som P, Brill B, et al. Dual tracer autoradiographic study of β-methyl-(1-^{14}C)-heptadecanoic acid and 15-p-(^{131}I)-iodophenyl-β-methylpentadecanoic acid in normotensive and hypertensive rats. *J Nucl Med* 1986; 27:1178–1183.
27. Olson RE. Myocardial metabolism in congestive heart failure. *J Chron Dis* 1959; 9:442–464.
28. Schelbert HR, Henze E, Sochor H, et al. Effects of substrate availability on myocardial C-11 palmitate kinetics by positron emission tomography in normal subjects and patients with ventricular dysfunction. *Am Heart J* 1986; 111:1055–1064.
29. Wrogemann K, Nylen EG. Mitochondrial calcium overloading in cardiomyopathic hamsters. *J Mol Cell Cardiol* 1978; 10:185–195.
30. Kobayashi A, Yamashita T, Kaneko M, Nishiyama T, Hayashi H, Yamazaki N. Effects of verapamil on experimental cardiomyopathy in the Bio 14.6 Syrian hamster. *J Am Coll Cardiol* 1987; 10:1128–1134.
31. Rellas JS, Corbett JR, Kulkarni PV, et al. Iodine-123 phenylpentadecanoic acid: detection of acute myocardial infarction and injury in dogs using an iodinated fatty acid and single-photon emission tomography. *Am J Cardiol* 1983; 52:1326–1332.
32. Kennedy PL, Corbett JR, Kulkarni PV, et al. Iodine 123-phenylpentadecanoic acid myocardial scintigraphy: usefulness in the identification of myocardial ischemia. *Circulation* 1986; 74:1007–1015.
33. Knapp FF Jr, Goodman MM, Callahan AP, Kirsch G. Radioiodinated 15-(p-iodophenyl)-3,3-dimethylpentadecanoic acid: a useful new agent to evaluate myocardial fatty acid uptake. *J Nucl Med* 1986; 27:521–531.
34. Kubota K, Som P, Brill AB, et al. Regional myocardial fatty acid uptake and blood-flow in cardiomyopathy: a quantitative autoradiographic study [Abstract]. *J Nucl Med* 1986; 27:933.